

# NUMERICAL MODELLING OF LOCALIZED FRACTURE OF INELASTIC SOLIDS IN DYNAMIC LOADING PROCESSES\*

TOMASZ ŁODYGOWSKI<sup>1</sup> AND PIOTR PERZYNA<sup>2,\*\*</sup>

<sup>1</sup>*Institute of Structural Engineering, Poznań University of Technology, Poznań, Poland*

<sup>2</sup>*Centre of Mechanics, Institute of Fundamental Technological Research, Polish Academy of Science, Warsaw, Poland*

## ABSTRACT

The main objective of the paper is the investigation of adiabatic shear band localized fracture phenomenon in inelastic solids during dynamic loading processes. This kind of fracture can occur as a result of an adiabatic shear band localization generally attributed to a plastic instability implied by microdamage and thermal softening during dynamic plastic flow processes.

By applying ideas of synergetics it can be shown that as a result of instability hierarchies a system is self-organized into a new shear band pattern system. This leads to the conclusion that inelastic solid body considered during the dynamics process becomes a two-phase material system. Particular attention is focussed on attempt to construct a physically and experimentally justified localized fracture theory that relates the kinetics of material failure on the microstructural level to continuum mechanics. The description of the microstructural damage process is based on dynamic experiments with carefully controlled load amplitudes and duration. The microdamage process has been treated as a sequence of nucleation, growth and coalescence of microcracks. The microdamage kinetics interacts with thermal and load changes to make failure of solids a highly rate, temperature and history-dependent, non-linear process.

The theory of thermoviscoplasticity is developed within the framework of the rate-type covariance material structure with a finite set of internal state variables. The theory takes into consideration the effects of microdamage mechanism and thermomechanical coupling. The dynamic failure criterion within localized shear band region is proposed. The relaxation time is used as a regularization parameter. Rate dependency (viscosity) allows the spatial differential operator in the governing equations to retain its ellipticity, and the initial-value problem is well-posed. The viscoplastic regularization procedure assures the unconditionally stable integration algorithm by using the finite element method. Particular attention is focused on the well-posedness of the evolution problem (the initial-boundary value problem) as well as on its numerical solutions. Convergence, consistency and stability of the discretized problem are discussed. The Lax equivalence theorem is formulated and conditions under which this theorem is valid are examined.

Utilizing the finite element method and ABAQUS system for regularized elasto-viscoplastic model the numerical investigation of the three-dimensional dynamic adiabatic deformation in a particular body at nominal strain rates ranging over  $10^3$ – $10^4$  s<sup>-1</sup> is presented. A thin shear band region of finite width which undergoes significant deformation and temperature rise has been determined. Its evolution until occurrence of final fracture has been simulated. Numerical results are compared with available experimental observation data. © 1997 John Wiley & Sons, Ltd.

*Int. J. Numer. Meth. Engng.*, **40**, 4137–4158 (1997)

No. of Figures: 7. No. of Tables: 0. No. of References: 34.

KEY WORDS: viscoplasticity; localization; regularization; micro-damage; localized fracture

\*Dedicated to Erwin Stein on the occasion of his 65th birthday

\*\*Correspondence to: P. Perzyna, Institute of Fundamental Technological Problems, Polish Academy of Sciences, Swietokrzyska 21, 00-049 Warsaw, Poland

Contract grant sponsor: Committee of Scientific Research; Contract grant number: 3P40403107

CCC 0029–5981/97/224137–22\$17.50

© 1997 John Wiley & Sons, Ltd.

Received 18 May 1996

Revised 10 February 1997

## 1. INTRODUCTION

In technological dynamical processes fracture can occur as a result of an adiabatic shear band localization generally attributed to a plastic instability generated by thermal softening during plastic deformation.

Hartley *et al.*,<sup>1</sup> Marchand and Duffy,<sup>2</sup> Marchand *et al.*,<sup>3</sup> and Cho *et al.*,<sup>4</sup> made microscopic observations of the shear band localization on the thin-walled steel tubes in a split Hopkinson torsion bar. Three different steels were tested. Dynamic deformation in shear was imposed to produce shear bands. It was found whenever the shear band led to fracture of the specimen, the fracture occurred by a process of void nucleation, growth and coalescence. No cleavage was observed on any fracture surface, including the most brittle of the steel tested.

This is presumably due to the thermal softening of the shear band material that results from the local temperature rise occurring during the deformation process.

In recent years Zbib and Jurban<sup>5</sup> have investigated numerically a three-dimensional problem involving the development of shear bands in a steel bar pulled in tension and Batra and Zhang<sup>6</sup> the three-dimensional dynamic thermomechanical deformations of a 4340 steel thin tube twisted in a split Hopkinson bar at nominal strain rate of 1000, 2500 and 25 000 s<sup>-1</sup>.

The main objective of the present paper is the application of a recently developed viscoplastic-damage type constitutive theory for high strain rate process and ductile fracture<sup>7,8</sup> to the problem of shear band localization and fracture of dynamically loaded thin-walled tubes experiencing strain rates ranging between 10<sup>3</sup>–10<sup>4</sup> s<sup>-1</sup>.

It has been proved that the localization of plastic deformation phenomenon in an elastic–viscoplastic solid body can arise only as the result of the reflection and interaction of waves. It has different character than that which occurs in a rate independent elasto-plastic solid body.<sup>7,9</sup> Rate dependency (viscosity) allows the spatial difference operator in the governing equations to retain its ellipticity and the initial value problem is well-posed. Viscosity introduces implicitly a length-scale parameter into the dynamical initial–boundary value problem and hence it implies that the localization region is diffused when compared with an inviscid plastic material. In the dynamical initial–boundary value problem the stress and deformation due to wave reflections and interactions are not uniformly distributed, and this kind of heterogeneity can lead to strain localization in the absence of geometrical or material irregularities. This kind of phenomenon has been recently noticed.<sup>10,11</sup>

The theory of viscoplasticity gives the possibility to obtain mesh-insensitive results in localization problems with respect to the width of the shear band and the wave reflection and interaction patterns.<sup>11</sup>

Since the rate independent plastic response is obtained as the limit case when the relaxation time  $T_m$  tends to zero<sup>7,9</sup> hence the theory of viscoplasticity offers the regularization procedure for the solution of the dynamical initial–boundary value problems with localization of plastic deformation.

In Section 2 a constitutive model is developed within a thermodynamic framework of the rate type material structure with internal state variables. Such important effects as the micro-damage mechanism and thermomechanical coupling are taken into consideration. It has been assumed that the intrinsic micro-damage mechanism consists of the nucleation, growth and coalescence of microvoids. The rate dependent evolution equation for the porosity parameter has been postulated.

In Section 3 the formulation of an adiabatic inelastic flow process is given. The Cauchy problem is investigated and the conditions which guarantee its well-posedness are examined.

Main features of rate dependent plastic model have been discussed. Particular attention has been focussed on the viscoplastic regularization procedure for the solution of the dynamical initial–boundary value problems with localization of plastic deformation. Some simplifications are introduced and a particular elastic–viscoplastic constitutive model for damaged solids is developed.

Numerical solutions of the initial–boundary value problem (evolution problem) are discussed Section 4. Mathematical formulation of the evolution problem is presented. Discretisation in space and time is proposed and convergence, consistency and stability are examined. The Lax equivalence theorem is formulated and conditions under which this theorem is valid are investigated.

Section 5 is devoted to the numerical investigation of the three-dimensional dynamic adiabatic deformations of a steel thin tube twisted in a split Hopkinson bar at nominal strain rates ranging  $10^3$ – $10^4$  s<sup>-1</sup>. A thin shear band region of finite width along the circumference of the tube which undergoes significant deformations and temperature rise has been determined. Its evolution until occurrence of fracture has been simulated. Numerical results are discussed and compared with available experimental observation data.

## 2. CONSTITUTIVE STRUCTURE

### 2.1. Rate type constitutive structure for an elastic–viscoplastic damaged material

The main objective is to develop the rate type constitutive structure for an elastic–viscoplastic material in which the effects of the micro-damage mechanism and thermomechanical coupling are taken into consideration.

Let us introduce the axioms as follows:

- (i) Axiom of the existence of the free energy function in the form

$$\psi = \hat{\psi}(\mathbf{e}, \mathbf{F}, \vartheta; \boldsymbol{\mu}) \tag{1}$$

where  $\mathbf{e}$  is the Eulerian strain tensor,  $\mathbf{F}$  the deformation gradient,  $\vartheta$  a temperature field and  $\boldsymbol{\mu}$  denotes the internal state variable vector.

- (ii) Axiom of objectivity (spatial covariance).<sup>12</sup> The constitutive structure should be invariant with respect to any diffeomorphism  $\xi: \mathcal{S} \rightarrow \mathcal{S}$ , where  $\mathcal{S}$  denotes the actual (spatial) configuration of a body  $\mathcal{B}$ .
- (iii) The axiom of entropy production. For any regular process  $\phi_t, \vartheta_t, \boldsymbol{\mu}_t$  of a body  $\mathcal{B}$  the constitutive functions are assumed to satisfy the reduced dissipation inequality

$$\frac{1}{\rho_{\text{Ref}}} \boldsymbol{\tau} : \mathbf{d} - (\eta \dot{\vartheta} + \dot{\psi}) - \frac{1}{\rho \vartheta} \mathbf{q} \cdot \text{grad } \vartheta \geq 0 \tag{2}$$

where  $\rho$  and  $\rho_{\text{Ref}}$  denote the mass density in the actual and reference configuration, respectively,  $\boldsymbol{\tau}$  is the Kirchhoff stress tensor,  $\mathbf{d} = \mathbf{d}^e + \mathbf{d}^p$  the rate of total deformation,  $\eta$  denotes the specific (per unit mass) entropy and  $\mathbf{q}$  is the heat vector field.

Let us postulate  $\boldsymbol{\mu} = (\zeta, \xi)$ , where  $\zeta$  denotes the new internal state vector which describes the dissipation effects generated by viscoplastic flow phenomena and  $\xi$  is the volume fraction porosity parameter and takes account for micro-damage mechanism.

Let us introduce the plastic potential function for damaged material in the form

$$f = J_2 + n\xi J_1^2, \quad \text{where} \quad J_1 = \tau^{ab}g_{ab}, \quad J_2 = \frac{1}{2} \tau'^{ab}\tau'^{cd}g_{ac}g_{bd} \tag{3}$$

$n = n(\vartheta)$  is the temperature dependent material function and  $\mathbf{g}$  denotes the metric tensor in  $\mathcal{S}$ .

Let us postulate the evolution equations as follows.<sup>†</sup> ( $L_v$  defines the Lie derivative with respect to the velocity field and the dot denotes the material derivative)

$$\mathbf{d}^p = \Lambda \mathbf{P}, \quad L_v \xi = \Lambda \mathbf{Z}, \quad \dot{\xi} = \Xi \tag{4}$$

where for the elastic–viscoplastic model of a material we assume<sup>7,9,13,14</sup>

$$\Lambda = \frac{1}{T_m} \langle \Phi(f - \kappa) \rangle \tag{5}$$

$T_m$  denotes the relaxation time for mechanical disturbances and  $\kappa$  is the isotropic work-hardening parameter,  $\Phi$  is the empirical overstress function and the bracket  $\langle \cdot \rangle$  defines the ramp function,  $\mathbf{P} = (1/2\sqrt{J_2})(\partial f/\partial \tau)$ , the material function  $\mathbf{Z}$  is intrinsically determined by the constitutive assumptions postulated and the scalar valued evolution function  $\Xi$  has to be determined. Thus, we have

$$P_{ab} = \frac{1}{2\sqrt{J_2}} \tau'^{cd}g_{ca}g_{db} + Ag_{ab}, \quad A = \frac{1}{\sqrt{J_2}} \eta \xi \tau^{ab}g_{ab} \tag{6}$$

The isotropic hardening-softening material function  $\kappa$  is assumed in the form as follows:

$$\kappa = \kappa_0^2 \{ q + (1 - q) \exp[-h(\vartheta)\varepsilon^p] \}^2 \left[ 1 - \left( \frac{\xi}{\xi^F} \right)^{1/2} \right] \tag{7}$$

where  $q = \kappa_1/\kappa_0$ ,  $\kappa_0$  and  $\kappa_1$  denote the yield and saturation stress of the matrix material (both can be temperature dependent functions), respectively,  $h = h(\vartheta)$  is the temperature dependent strain hardening function for the matrix material,  $\varepsilon^p = \int_0^t (\frac{2}{3} \mathbf{d}^p : \mathbf{d}^p)^{1/2} dt$  is the equivalent plastic deformation,  $\xi^F$  denotes the value of porosity at which the incipient fracture occurs; the overstress viscoplastic function  $\Phi$  is postulated in the form<sup>13,14</sup>

$$\Phi(f - \kappa) = \left( \frac{f}{\kappa} - 1 \right)^m, \quad \text{where } m = 1, 3, 5, \dots \tag{8}$$

The axioms (i)–(iii) and the evolution equations (4) lead to the rate equations as follows:

$$\begin{aligned} L_v \tau &= \mathcal{L}^e : \mathbf{d} - \mathcal{L}^{th} \dot{\vartheta} - [(\mathcal{L}^e + \mathbf{g}\boldsymbol{\tau} + \boldsymbol{\tau}\mathbf{g}) : \mathbf{P}] \frac{1}{T_m} \left\langle \Phi \left( \frac{f}{\kappa} - 1 \right)^m \right\rangle \\ \dot{\vartheta} &= - \frac{1}{\rho c_p} \text{div } \mathbf{q} + \frac{\vartheta}{c_p \rho_{Ref}} \frac{\partial \tau}{\partial \vartheta} : \mathbf{d} + \frac{\chi^*}{\rho c_p} \boldsymbol{\tau} : \mathbf{d}^p + \frac{\chi^{**}}{\rho c_p} \dot{\xi} \end{aligned} \tag{9}$$

<sup>†</sup> For precise definition of the finite elasto-plastic deformation see Perzyna<sup>9</sup>

where

$$\mathcal{L}^e = \rho_{\text{Ref}} \frac{\partial^2 \hat{\psi}}{\partial \mathbf{e}^2}, \quad \mathcal{L}^{\text{th}} = -\rho_{\text{Ref}} \frac{\partial^2 \hat{\psi}}{\partial \mathbf{e} \partial \vartheta}, \quad c_p = -\vartheta \frac{\partial^2 \hat{\psi}}{\partial \vartheta^2} \tag{10}$$

$\chi^*$  and  $\chi^{**}$  are the irreversibility coefficients.

To make possible numerical investigation of the three-dimensional dynamic adiabatic deformations of a body for different ranges of strain rate we introduce some simplifications of the constitutive model.

- (i) By analogy with the infinitesimal theory of elasticity we postulate linear elastic properties of the material, i.e.

$$(\mathcal{L}^e)^{abcd} = \bar{G}(g^{ac}g^{db} + g^{cb}g^{da}) + (\bar{K} - \frac{2}{3}\bar{G})g^{ab}g^{cd} + \tau^{bd}g^{ac} \tag{11}$$

where  $\bar{G}$  and  $\bar{K}$  denote the shear and bulk modulus of damaged material, respectively.<sup>15</sup>

- (ii) It is assumed that

$$\mathcal{L}^{e^{-1}} : \mathcal{L}^{\text{th}} = \theta \mathbf{g} \tag{12}$$

where  $\theta$  is the thermal expansion coefficient in elastic range.

Because of the presence of microvoids, the elastic shear and bulk moduli  $\bar{G}$  and  $\bar{K}$ , respectively, are assumed to be degraded according to the model<sup>16</sup>

$$\bar{G} = G(1 - \xi) \left( 1 - \frac{6K + 12G}{9K + 8G} \xi \right), \quad \bar{K} = \frac{4GK(1 - \xi)}{4G + 3K\xi} \tag{13}$$

where  $G$  and  $K$  are the elastic moduli of unvoided material.

### 2.2. Intrinsic micro-damage process

The intrinsic micro-damage process consists of nucleation, growth and coalescence of microvoids (microcracks). Recent experimental observation results<sup>17</sup> have shown that coalescence mechanism can be treated as nucleation and growth process on a smaller scale. This conjecture simplifies very much the description of the intrinsic micro-damage process by taking account only of the nucleation and growth mechanisms. Then the porosity or the void volume fraction parameter  $\xi$  can be determined by  $\dot{\xi} = (\dot{\xi})_{\text{nuc}} + (\dot{\xi})_{\text{grow}}$ .

Physical considerations<sup>18,15</sup> have shown that the nucleation of microvoids in dynamic loading processes which are characterized by very short time duration is governed by the thermally activated mechanism. Based on this heuristic suggestion we postulate for rate dependent plastic flow

$$(\dot{\xi})_{\text{nuc}} = \frac{1}{T_m} h^*(\xi, \vartheta) \left[ \exp \frac{m^*(\vartheta) |\sigma - \sigma_N(\xi, \vartheta, \varepsilon^p)|}{k\vartheta} - 1 \right] \tag{14}$$

where  $k$  denotes the Boltzmann constant,  $h^*(\xi, \vartheta)$  represents a void nucleation material function which is introduced to take account of the effect of microvoid interaction,  $m^*(\vartheta)$  is a temperature dependent coefficient,  $\sigma = (1/3)J_1$  is the mean stress and  $\sigma_N(\xi, \vartheta, \varepsilon^p)$  is the porosity, temperature and equivalent plastic strain dependent threshold stress for microvoid nucleation.

For the growth mechanism we postulate<sup>15,19–22</sup>

$$(\dot{\xi})_{\text{grow}} = \frac{1}{T_m} \frac{g^*(\xi, \vartheta)}{\sqrt{\kappa}} [\sigma - \sigma_{\text{eq}}(\xi, \vartheta, \varepsilon^p)] \tag{15}$$

where  $T_m \sqrt{\kappa}$  denotes the dynamic viscosity of a material,  $g^*(\xi, \vartheta)$  represents a void growth material function and takes account for void interaction and  $\sigma_{\text{eq}}(\xi, \vartheta, \varepsilon^p)$  is the porosity, temperature and equivalent plastic strain-dependent void growth threshold mean stress.

Equations (14) and (15) determine the evolution function  $\Xi$  postulated in equation (4)<sub>3</sub>.

### 2.3. Fracture criterion

We base the fracture criterion on the evolution of the porosity internal state variable.

Let us assume that for  $\xi = \xi^F$  catastrophe takes place,<sup>23</sup> i.e.

$$\kappa = \hat{\kappa}(\varepsilon^p, \vartheta, \xi)|_{\xi=\xi^F} = 0 \tag{16}$$

It means that for  $\xi = \xi^F$  the material loses its stress carrying capacity. The condition (16) describes the main feature observed experimentally that the load tends to zero at the fracture point. It is noteworthy that the isotropic hardening–softening material function  $\hat{\kappa}$  proposed in particular form (7) satisfies the fracture criterion (16).

## 3. ADIABATIC INELASTIC FLOW PROCESS

### 3.1. Formulation of an adiabatic inelastic flow process

Let us define an adiabatic inelastic flow process as follows.<sup>7,9</sup> Find  $\phi, \mathbf{v}, \rho_M, \boldsymbol{\tau}, \xi$  and  $\vartheta$  as function of  $t$  and  $\mathbf{x}$  such that

(i) the field equations

$$\begin{aligned} \dot{\phi} &= \mathbf{v}, \\ \dot{\mathbf{v}} &= \frac{1}{\rho_M^0(1 - \xi_0)} \left( \frac{\boldsymbol{\tau}}{\rho_M} \text{grad } \rho_M + \text{div } \boldsymbol{\tau} - \frac{\boldsymbol{\tau}}{1 - \xi} \text{grad } \xi \right) \\ \dot{\rho}_M &= \frac{\rho_M}{1 - \xi} \Xi - \rho_M \text{div } \mathbf{v}, \\ \dot{\boldsymbol{\tau}} &= \left[ \mathcal{L}^e - \frac{1}{c_p \rho_{\text{Ref}}} \vartheta \mathcal{L}^{\text{th}} \frac{\partial \boldsymbol{\tau}}{\partial \vartheta} \right] : \text{sym } D\mathbf{v} + 2 \text{sym} \left( \boldsymbol{\tau} : \frac{\partial \mathbf{v}}{\partial \mathbf{x}} \right) \\ &\quad - \left[ \left( \frac{\lambda^*}{\rho_M(1 - \xi)c_p} \mathcal{L}^{\text{th}} \boldsymbol{\tau} + \mathcal{L}^e + \mathbf{g}\boldsymbol{\tau} + \boldsymbol{\tau}\mathbf{g} \right) : \mathbf{P} \right] \frac{1}{T_m} \left\langle \left( \frac{f}{\kappa} - 1 \right)^m \right\rangle \\ &\quad - \frac{\lambda^{**} \mathcal{L}^{\text{th}}}{\rho_M(1 - \xi)c_p} \Xi \\ \dot{\xi} &= \Xi \end{aligned}$$

$$\begin{aligned} \dot{g} = & \frac{\vartheta}{c_p \rho_{\text{Ref}}} \frac{\partial \boldsymbol{\tau}}{\partial \vartheta} : \text{sym } D\mathbf{v} + \frac{\chi^*}{\rho_M(1-\xi)c_p} \boldsymbol{\tau} : \mathbf{P} \frac{1}{T_m} \left\langle \left( \frac{f}{\kappa} - 1 \right)^m \right\rangle \\ & + \frac{\chi^{**}}{\rho_M(1-\xi)c_p} \Xi; \end{aligned} \tag{17}$$

(ii) the boundary conditions

- (a) displacement  $\phi$  is prescribed on a part  $\partial_\phi$  of  $\partial\phi(\mathcal{B})$  and tractions  $(\boldsymbol{\tau} \cdot \mathbf{n})^a$  are prescribed on part  $\partial_\tau$  of  $\partial\phi(\mathcal{B})$ , where  $\partial_\phi \cap \partial_\tau = 0$  and  $\overline{\partial_\phi \cup \partial_\tau} = \partial\phi(\mathcal{B})$ ;
- (b) heat flux  $\mathbf{q} \cdot \mathbf{n} = 0$  is prescribed on  $\partial\phi(\mathcal{B})$ ;

(iii) the initial conditions

$\phi, \mathbf{v}, \sigma_M, \vartheta, \xi$  and  $\boldsymbol{\tau}$  are given at each particle  $X \in \mathcal{B}$  at  $t = 0$ ;

are satisfied.

In the field equations (17)  $\rho_M$  and  $\rho_M^0$  denote the actual and reference mass density of the matrix material, respectively,  $\xi_0$  is the initial porosity of a material and  $D\mathbf{v}$  denotes the spatial velocity gradient.

Equation (17)<sub>1</sub> represents the kinematic relation. For damaged solid body the mass density  $\rho$  can be approximated by  $\rho = \rho_M(1 - \xi)$  and  $\rho_{\text{Ref}} = \rho_M^0(1 - \xi_0)$ . When the Kirchhoff stress tensor  $\boldsymbol{\tau} = (\rho/\rho_{\text{Ref}}) \boldsymbol{\sigma}$  ( $\boldsymbol{\sigma}$  denotes the Cauchy stress tensor) is used as measure of stress then the Cauchy equation of motion  $\rho \dot{\mathbf{v}} = \text{div } \boldsymbol{\sigma}$  takes the form of equation (17)<sub>2</sub>. Equation (17)<sub>3</sub> expresses the conservation of mass for damaged solid body, equation (17)<sub>4</sub> is obtained from (9)<sub>1</sub> by substituting (9)<sub>2</sub> with  $\mathbf{q} = 0$  for adiabatic process and using the relation  $\mathbf{d} = \text{sym } D\mathbf{v}$ . Equation (17)<sub>5</sub> defines the evolution equation for the porosity parameter  $\xi$  and equation (17)<sub>6</sub> is obtained from (9)<sub>2</sub> for adiabatic process, i.e. for  $\mathbf{q} = 0$ .

### 3.2. The Cauchy problem

Let us consider the Cauchy problem<sup>7,24,25</sup>

$$\dot{\boldsymbol{\varphi}} = \mathcal{A}(t, \boldsymbol{\varphi})\boldsymbol{\varphi} + \mathbf{f}(t, \boldsymbol{\varphi}), \quad t \in [0, t_f], \quad \boldsymbol{\varphi}(0) = \boldsymbol{\varphi}^0 \tag{18}$$

where  $\mathcal{A}$  is a spatial differential operator and  $\mathbf{f}$  is a non-linear function, both defined by the governing equations (17).

In order to examine the existence, uniqueness and well-posedness of the Cauchy problem (18) let us assume that the spatial differential operator  $\mathcal{A}$  has domain  $\mathcal{D}(\mathcal{A})$  and range  $\mathcal{R}(\mathcal{A})$ , both contained in a real Banach space  $E$  and the nonlinear function  $\mathbf{f}$  is as follows  $\mathbf{f}: E \rightarrow E$ . To investigate the existence as well as the stability of solutions to (18) it is necessary to characterize their properties without actually constructing the solutions. This can be done by considering the properties of a nonlinear semi-group because if the operator  $\mathcal{A} + \mathbf{f}(\cdot)$  generates a nonlinear semi-group  $\{\mathbb{F}_t^*; t \geq 0\}$ , then a solution to (18) starting at  $t = 0$  from any element  $\boldsymbol{\varphi}^0 \in \mathcal{D}(\mathcal{A})$  is given by

$$\boldsymbol{\varphi}(t, \mathbf{x}) = \mathbb{F}_t^* \boldsymbol{\varphi}^0(\mathbf{x}) \quad \text{for } t \in [0, t_f] \tag{19}$$

We say the problem (18) is well posed if  $\mathbb{F}_t^*$  is continuous (in the topology on  $\mathcal{D}(\mathcal{A})$  and  $\mathcal{R}(\mathcal{A})$  assumed) for each  $t \in [0, t_f]$ .

Let us postulate as follows:

(i) the strong ellipticity condition in the form:

$$\mathbb{E} = \mathcal{L}^e - \frac{1}{c_p \rho_{\text{Ref}}} g_{\mathcal{L}^{\text{th}}} \frac{\partial \tau}{\partial \mathcal{G}} \tag{20}$$

is strongly elliptic (at a particular deformation  $\phi$ ) if there is an  $\varepsilon > 0$  such that

$$\mathbb{E}^{abcd} \zeta_a \zeta_c \xi_b \xi_d \geq \varepsilon \|\zeta\|^2 \|\xi\|^2 \tag{21}$$

for all vectors  $\zeta$  and  $\xi \in \mathbb{R}^3$ ;

(ii) for positive numbers  $\lambda_f^1$  and  $\lambda_f^2$  and for  $T_m > 0$

$$\mathbf{f}(t, \boldsymbol{\varphi}) \in E, \quad \|\mathbf{f}(t, \boldsymbol{\varphi})\|_E \leq \lambda_f^1, \quad \|\mathbf{f}(t, \boldsymbol{\varphi}') - \mathbf{f}(t, \boldsymbol{\varphi})\|_E \leq \lambda_f^2 \|\boldsymbol{\varphi}' - \boldsymbol{\varphi}\|_E \tag{22}$$

and

$$t \rightarrow \mathbf{f}(t, \boldsymbol{\varphi}) \in E \quad \text{is continuous} \tag{23}$$

Using the results<sup>12,26</sup> it is possible to show<sup>7,9</sup> that the conditions (i) and (ii) guarantee the existence of (locally defined) evolution operators  $\mathbb{F}_t^*$ :  $E \rightarrow E$  that are continuous in all variables. In other words the solution of the Cauchy problem (18) in the form (19) exists, is unique and well-posed.

#### 4. NUMERICAL SOLUTION OF THE INITIAL-BOUNDARY VALUE PROBLEM (EVOLUTION PROBLEM)

##### 4.1. Formulation of the evolution problem

Find  $\boldsymbol{\varphi}$  as function of  $t$  and  $\mathbf{x}$  satisfying<sup>‡</sup>

$$\left. \begin{aligned} \text{(i)} \quad & \dot{\boldsymbol{\varphi}} = \mathcal{A}(t, \boldsymbol{\varphi})\boldsymbol{\varphi} + \mathbf{f}(t, \boldsymbol{\varphi}); \\ \text{(ii)} \quad & \boldsymbol{\varphi}(0) = \boldsymbol{\varphi}^0(\mathbf{x}); \\ \text{(iii)} \quad & \text{The boundary conditions} \\ & \text{(e.g. as have been postulated in Section 3.1)} \end{aligned} \right\} \tag{24}$$

A strict solution of (24) with  $\mathbf{f}(t, \boldsymbol{\varphi}) \equiv 0$  (i.e. the homogeneous evolution problem) is defined as a function  $\boldsymbol{\varphi}(t) \in E$  (a Banach space) such that

$$\boldsymbol{\varphi}(t) \in \mathcal{D}(\mathcal{A}), \quad \text{for all } t \in [0, t_f], \tag{25}$$

$$\lim_{\Delta t \rightarrow 0} \left\| \frac{\boldsymbol{\varphi}(t + \Delta t) - \boldsymbol{\varphi}(t)}{\Delta t} - \mathcal{A}\boldsymbol{\varphi}(t) \right\|_E = 0 \quad \text{for all } t \in [0, t_f]$$

The boundary conditions are taken care of by restricting the domain  $\mathcal{D}(\mathcal{A})$  to elements of  $E$  that satisfy those conditions; they are assumed to be linear and homogeneous, so that the set  $\mathbf{S}$  of all  $\boldsymbol{\varphi}$  that satisfy them is a linear manifold;  $\mathcal{D}(\mathcal{A})$  is assumed to be contained in  $\mathbf{S}$ .

<sup>‡</sup> We shall follow here some fundamental results<sup>27-30</sup>



The choice of the Banach space  $E$ , as well as the domain of  $\mathcal{A}$ , is an essential part of the formulation of the evolution problem.

4.2. *Well-posedness of the evolution problem*

The homogeneous evolution problem (i.e. for  $\mathbf{f} \equiv 0$ ) is called well-posed (in the sense of Hadamard) if it has the following properties:<sup>27</sup>

- (i) The strict solutions are uniquely determined by their initial elements;
- (ii) The set  $Y$  of all initial elements of strict solutions is dense in the Banach space  $E$ ;
- (iii) For any finite interval  $[0, t_0]$ ,  $t_0 \in [0, t_f]$  there is a constant  $K = K(t_0)$  such that every strict solution satisfies the inequality

$$\|\boldsymbol{\varphi}(t)\| \leq K \|\boldsymbol{\varphi}^0\|, \quad \text{for } 0 \leq t \leq t_0 \tag{26}$$

The inhomogeneous evolution problem (24) will be called well-posed if it has a unique solution for all reasonable choices of  $\boldsymbol{\varphi}^0$  and  $\mathbf{f}(t, \boldsymbol{\varphi})$  and if the solution depends continuously, in some sense, on those choices.

It is possible to show<sup>27</sup> that strict solutions exists for sets of  $\boldsymbol{\varphi}^0$  and  $\mathbf{f}(\cdot)$  that are dense in  $E$  and  $E_1$  (a new Banach space), respectively.

4.3. *Discretization in space and time*

We must approximate (24) twice. First, when  $E$  is infinite dimensional, we must replace  $\mathcal{A}$  by an operator  $\mathcal{A}_h$  which operates in a finite dimensional space  $V_h \subset E$ , where, in general,  $h > 0$  represents a discretisation step in space, such that  $\dim(V_h) \rightarrow \infty$  as  $h \rightarrow 0$ . Second, we must discretise in time, that is to say choose a sequence of moments  $t_n$  (for example  $t_n = n\Delta t$ , where  $\Delta t$  is time step) at which we shall calculate the approximate solution.

Let us introduce the following semi-discretized (discrete in space) problem.<sup>28</sup>

$$\left. \begin{aligned} &\text{Find } \boldsymbol{\varphi}_h \in \mathcal{C}^0([0, t_0]; V_h) \text{ (}\mathcal{C}^0 \text{ denotes the space of functions} \\ &\text{continuous on } ([0, t_0], V_h)) \text{ satisfying} \\ &\frac{d\boldsymbol{\varphi}_h(t)}{dt} = \mathcal{A}_h \boldsymbol{\varphi}_h(t) + \mathbf{f}_h(t) \\ &\boldsymbol{\varphi}_h(0) = \boldsymbol{\varphi}_{0,h} \end{aligned} \right\} \tag{27}$$

The operator  $\mathcal{A}_h$  for the finite element method can be obtained by a variational formulation approach. The discrete equations are obtained by the Galerkin method at particular points in the domain.

Finally, we shall define a method allowing us to calculate  $\boldsymbol{\varphi}_h^n \in V_h$ , an approximation to  $\varphi_h(t_n)$  starting from  $\boldsymbol{\varphi}_h^{n-1}$  (we limit ourselves to a two-level scheme). Then we can write<sup>28</sup>

$$\boldsymbol{\varphi}_h^{n+1} = C_h(\Delta t) \boldsymbol{\varphi}_h^n + \Delta t \mathbf{f}_h^n, \quad \boldsymbol{\varphi}_h^0 = \boldsymbol{\varphi}_{0,h} \tag{28}$$

where we introduce the operator  $C_h(\Delta t) \in \mathcal{L}(V_h)$  ( $\mathcal{L}$  is the set of continuous linear mapping of  $V_h$  with values in  $V_h$ ) and where  $\mathbf{f}_h^n$  approximates  $\mathbf{f}_h(t_n)$ .

We shall always assume that the evolution problem (24) is well-posed and there exists a projection  $R_h$  of  $E$  into  $V_h$  such that

$$\lim_{h \rightarrow 0} |R_h \boldsymbol{\varphi} - \boldsymbol{\varphi}|_E = 0 \quad \forall \boldsymbol{\varphi} \in E \tag{29}$$

4.4. *Convergence, consistency and stability*

The first fundamental question is that of the convergence, when  $h$  and  $\Delta t$  tend to zero, of the sequence  $\{\boldsymbol{\varphi}_h^n\}$ , the solution (28), towards the function  $\boldsymbol{\varphi}(t)$ , the solution of (24). Let us restrict our consideration, for the moment, to the case where  $\mathbf{f}(t) \equiv 0$ .

*Definition 1.* The scheme defined by (28) will be called convergent if the condition<sup>28</sup>

$$\boldsymbol{\varphi}_{0,h} \rightarrow \boldsymbol{\varphi}^0 \quad \text{as } h \rightarrow 0 \tag{30}$$

implies that

$$\boldsymbol{\varphi}_h^n \rightarrow \boldsymbol{\varphi}(t) \quad \text{as } \Delta t \rightarrow 0, \quad n \rightarrow \infty \quad \text{with } n\Delta t \rightarrow t \tag{31}$$

for all  $t \in ]0, t_0[$ ,  $t_0 \in [0, t_f]$ , where  $\boldsymbol{\varphi}_h^n$  is defined by (28) and  $\boldsymbol{\varphi}(t)$  is the solution of (24). All this holds for arbitrary  $\boldsymbol{\varphi}^0$ .

The study of the convergence of an approximation scheme involves two fundamental properties of the scheme, consistency and stability.<sup>28</sup>

*Definition 2.* The scheme defined by (28) will be called consistent with equation (24) if there exists a subspace  $Y \subset E$  dense in  $E$ , such that for every  $\boldsymbol{\varphi}(t)$  which is a solution of (24) with  $\boldsymbol{\varphi}^0 \in Y$  (and  $\mathbf{f} \equiv 0$ ) we have<sup>28</sup>

$$\lim_{h \rightarrow 0, \Delta t \rightarrow 0} \left| \frac{C_h(\Delta t)R_h \boldsymbol{\varphi}(t) - \boldsymbol{\varphi}(t)}{\Delta t} - \mathcal{A} \boldsymbol{\varphi}(t) \right|_E = 0 \tag{32}$$

In definitions 1 and 2 there occur two parameters  $h$  and  $\Delta t$ . It may be that the scheme is not stable (or not convergent) unless  $\Delta t$  and  $h$  satisfy supplementary hypotheses of the type  $\Delta t/h^\alpha \leq \text{constant}$ ,  $\alpha < 0$ , in which case we call the scheme *conditionally stable*. If the scheme is stable for arbitrary  $h$  and  $\Delta t$  we say that it is *unconditionally stable*.

These schemes reflect so called explicit and implicit types of the integration procedure in a particular numerical implementation.

*Definition 3.* The scheme defined by (28) is called stable, if there exists a constant  $K \geq 1$  independent of  $h$  and  $\Delta t$  such that<sup>28,30</sup>

$$\|C_h(\Delta t)^n R_h\|_{\mathcal{L}(E)} \leq K \quad \forall n, \Delta t \quad \text{satisfying } n\Delta t \leq t_0 \tag{33}$$

4.5. *The equivalence theorem*

We can now state the Lax equivalence theorem.<sup>28,30,31</sup>

*Theorem.* Suppose that the evolution problem (24) is well-posed for  $t \in [0, t_0]$  and that it is approximated by the scheme (28). Then the scheme is convergent if and only if the assertions of consistency (32) and stability (33) are satisfied.

The proof of the Lax equivalence theorem can be found in Dautray and Lions.<sup>4</sup>

*Remark.* Let us consider the evolution problem (24) with

$$\mathbf{f}(t, \boldsymbol{\varphi}) \neq 0 \tag{34}$$

and  $\boldsymbol{\varphi}^0 = 0$ , and also the corresponding approximation (28). We have

$$\boldsymbol{\varphi}_h^{n+1} = \Delta t \sum_{j=1}^n [C_h(\Delta t)]^{n-j} \mathbf{f}_h^j \tag{35}$$

If  $\mathcal{A}$  is the infinitesimal generator of a semigroup  $\{\mathbb{F}(t)\}$  we can write

$$\boldsymbol{\varphi}(t) = \int_0^t \mathbb{F}(t-s) \mathbf{f}(s) ds \tag{36}$$

Under suitable hypotheses on the convergence of  $\mathbf{f}_h^j$  to  $\mathbf{f}(j\Delta t)$  we can show that expression (35) converges to (36) if the scheme is stable and consistent.

4.6. Application to an adiabatic inelastic flow process

The evolution problem (24) describes an adiabatic inelastic flow process formulated in Section 3.1 provided

$$\boldsymbol{\varphi} = \begin{bmatrix} \phi \\ \mathbf{v} \\ \rho_M \\ \boldsymbol{\tau} \\ \xi \\ \vartheta \end{bmatrix}, \quad \mathbf{f} = \begin{bmatrix} \mathbf{v} \\ 0 \\ \frac{\rho_M}{1-\xi} \boldsymbol{\Xi} \\ \left[ \left( \frac{\chi^*}{\rho_M(1-\xi)c_p} \mathcal{L}^{\text{th}} \boldsymbol{\tau} + \mathcal{L}^e + \mathbf{g}\boldsymbol{\tau} + \boldsymbol{\tau}\mathbf{g} \right) : \mathbf{P} \right] \frac{1}{T_m} \left\langle \left( \frac{f}{\kappa} - 1 \right)^m \right\rangle - \frac{\chi^{**}\boldsymbol{\Xi}}{\rho_M(1-\xi)c_p} \mathcal{L}^{\text{th}} \\ \boldsymbol{\Xi} \\ \frac{\chi^*}{\rho_M(1-\xi)c_p} \boldsymbol{\tau} : \mathbf{P} \frac{1}{T_m} \left\langle \left( \frac{f}{\kappa} - 1 \right)^m \right\rangle + \frac{\chi^{**}}{\rho_M(1-\xi)c_p} \boldsymbol{\Xi} \end{bmatrix}$$

$$\mathcal{A} = \begin{bmatrix} 0 & 0 & 0 & 0 & 0 & 0 \\ 0 & 0 & \frac{1}{\rho_M^0(1-\xi_0)} \frac{\boldsymbol{\tau}}{\rho_M} \text{grad} & \frac{\text{div}}{\rho_M^0(1-\xi_0)} & \frac{\boldsymbol{\tau} \text{grad}}{\rho_M^0(1-\xi_0)(1-\xi)} & 0 \\ 0 & -\rho_M \text{div} & 0 & 0 & 0 & 0 \\ 0 & \boldsymbol{\Xi} : \text{sym} \frac{\partial}{\partial \mathbf{x}} + 2 \text{sym} \left( \boldsymbol{\tau} : \frac{\partial}{\partial \mathbf{x}} \right) & 0 & 0 & 0 & 0 \\ 0 & 0 & 0 & 0 & 0 & 0 \\ 0 & \frac{\vartheta}{c_p \rho_{\text{Ref}}} \frac{\partial \boldsymbol{\tau}}{\partial \vartheta} : \text{sym} \frac{\partial}{\partial \mathbf{x}} & 0 & 0 & 0 & 0 \end{bmatrix} \tag{37}$$

It is noteworthy that the spatial operator  $\mathcal{A}$  has the same form as in elastodynamics of damaged material while all dissipative effects generated by viscoplastic flow phenomena influence the process through the nonlinear function  $\mathbf{f}$ .

Let us consider first undamaged material (i.e. we assume  $\Xi \equiv 0$ ). For this case the spatial operator  $\mathcal{A}$  has strictly the form as in elastodynamics. Then, for the proof of the well-posedness of the homogeneous evolution problem (for  $\mathbf{f} \equiv 0$ ) we can use the results obtained in elastodynamics. Next, we can extend the results to elasto-viscoplasticity by considering the non-homogeneous evolution problem (when  $\mathbf{f} \neq 0$ ) and by superposing suitable smoothness assertions for the nonlinear function  $\mathbf{f}$ .<sup>7,9,29</sup>

It is sufficient to assume for the non-linear function  $\mathbf{f}$  the assertions as have been postulated by (22) and (23). These conditions are satisfied provided we assume:

- (i) The yield function  $f = f(J_1, J_2, \xi, \vartheta)$  is smooth in the stress space and depends continuously on  $\xi$  and  $\vartheta$ . The particular form of the yield function (3) satisfies this assertion if the material function  $n = n(\vartheta)$  is continuous.
- (ii) The isotropic hardening material function  $\kappa = \hat{\kappa}(\varepsilon^p, \xi, \vartheta)$  is a continuous function in all variables. The particular form of  $\hat{\kappa}$  assumed by (7) satisfies this condition for smooth  $h = h(\vartheta)$ .
- (iii) The overstress viscoplastic function  $\Phi = \Phi(f - \kappa)$  is absolutely continuous. It means that it can be postulated in the form (8).
- (iv) The evolution function  $\Xi$  is absolutely continuous. This assertion is satisfied by the nucleation and growth terms (14) and (15) provided the material function  $h^*$ ,  $m^*$ ,  $\sigma_N$ ,  $g^*$  and  $\sigma_{eq}$  are sufficiently smooth.

This analysis clearly shows how the constitutive modelling of the material is directly related to the well-posedness of the evolution problem (i.e. the initial boundary value problem).

## 5. SHEAR BAND LOCALIZATION FRACTURE

### 5.1. Formulation of the initial-boundary value problem for a thin steel tube

Cho, *et al.*<sup>4</sup> tested the specimens machined in the shape of thin-walled tubes with integral hexagonal flanges for gripping. Torsional loading at high strain rates was applied in a torsional Kolsky bar (split-Hopkinson bar).

We idealize the initial-boundary value problem<sup>6</sup> by assuming the specimen in the shape of thin-walled tube.

The initial conditions are taken in the form

$$\begin{aligned} \phi(\mathbf{x}, 0) = 0, \quad \mathbf{v}(\mathbf{x}, 0) = 0, \quad \rho(\mathbf{x}, 0) = \rho_{Ref} = \rho_M^0(1 - \xi_0) \\ \tau(\mathbf{x}, 0) = 0, \quad \xi(\mathbf{x}, 0) = \xi_0, \quad \vartheta(\mathbf{x}, 0) = \vartheta_0 = \text{constant in } \mathcal{B} \end{aligned} \quad (38)$$

That is, the body is initial at rest, is stress free at a uniform temperature  $\vartheta_0$  and the initial porosity at every material point is  $\xi_0$ .

For the boundary conditions, we assume

$$\boldsymbol{\tau} \cdot \mathbf{n} = 0 \text{ on the inner and outer surfaces of the tube}$$

$$\mathbf{q} \cdot \mathbf{n} = 0 \Rightarrow \text{grad } \vartheta \cdot \mathbf{n} = 0 \text{ on all bounding surfaces}$$

$$\mathbf{v}(x_1, x_2, 0, t) = 0, \mathbf{v}(x_1, x_2, L, t) = \omega^*(t)(x_1^2 + x_2^2)^{1/2} \mathbf{n}^* \tag{39}$$

where  $\mathbf{n}$  is a unit outward normal to the respective surfaces,  $\omega^*(t)$  is the angular speed of the end surface  $x_3 = L$  of the tube, and  $\mathbf{n}^*$  is a unit vector tangent to the surface  $x_3 = L$ . It is assumed that

$$\omega^*(t) = \begin{cases} \omega_0^* t/40, & 0 \leq t \leq 40 \mu\text{s}, \\ \omega_0^* & t > 40 \mu\text{s} \end{cases} \tag{40}$$

The rise time of 40  $\mu\text{s}$  is typical for torsional tests done in a split Hopkinson bar.<sup>6</sup>

5.2. Numerical computation and discussion of the results

The aforestated initial-boundary value problem of twisting the thin-walled steel tube has been numerically treated by using the general purpose finite element code ABAQUS.

After a discussion and the estimation of computational efficiency<sup>32</sup> the half of the specimen (only the thin walled cylinder, cf. Figure 1) is modelled via multilayer, 4-noded shell elements. Five integration Simpson's points in the thickness direction are used at each of four Gauss points of shell reduced integration element (S4R). The other models which were analysed (for example 3-D models) drove to huge numerical problems that exceeded 60,000 degrees of freedom. This dimension of the dynamically formulated problem does not guarantee the possibility to obtain the results in reasonable time even using very powerful computers. In circumferential direction the model consists of 24 segments with 10 elements on the depth of the half of a specimen, cf. Figure 2.

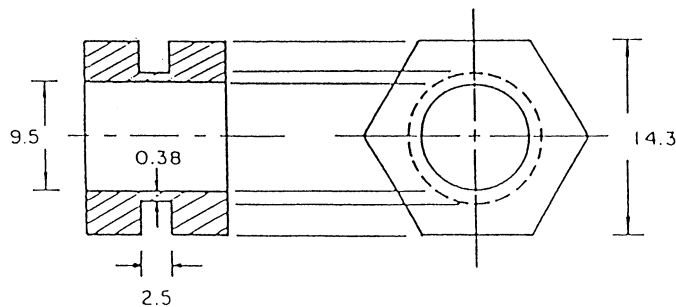


Figure 1. Details of the specimen with hexagonal mounting flanges used in the torsional Kolsky bar experiment<sup>32</sup> (all dimensions are in millimeters)

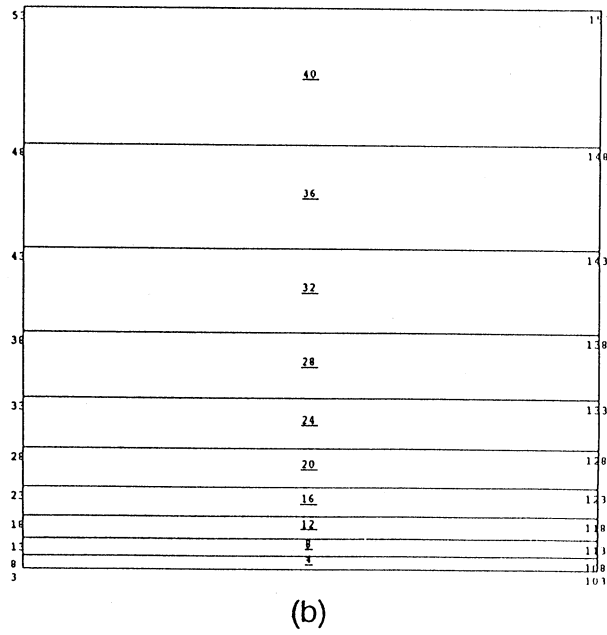
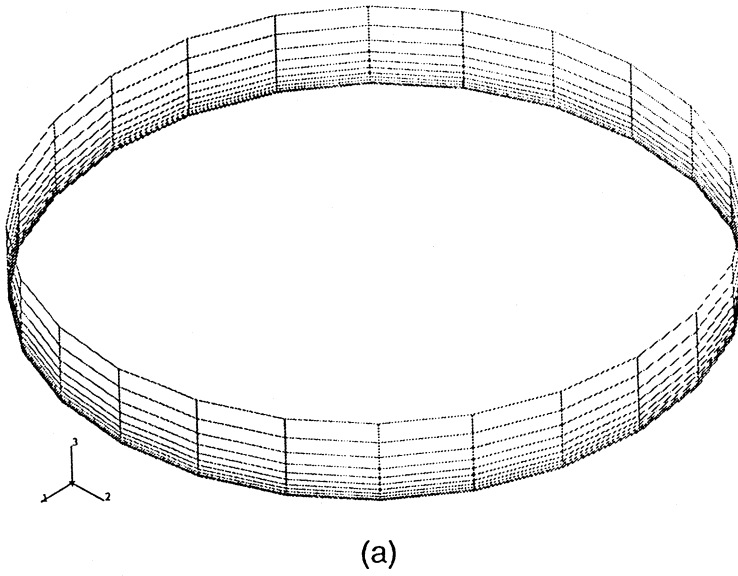


Figure 2. Layer shell divided into 24 segments with 10 elements on the depth

To avoid the reflection of waves and to model the influence of the rest of the specimen (cf. Figure 1) it has been postulated that the additional spring and mass elements are taken into consideration.

The rigidity of the spring and the value of the additional mass have been established in such a way to reflect the behaviour of the remaining part of the specimen.

Basically, after several tests we decided to use explicit method of integration of the nonlinear dynamic equations which, however conditionally stable and requires large number of time increments, in the case under consideration is more efficient than implicit one. To be sure that the numerical scheme is convergent the conditions (32) and (33) have been estimated numerically.

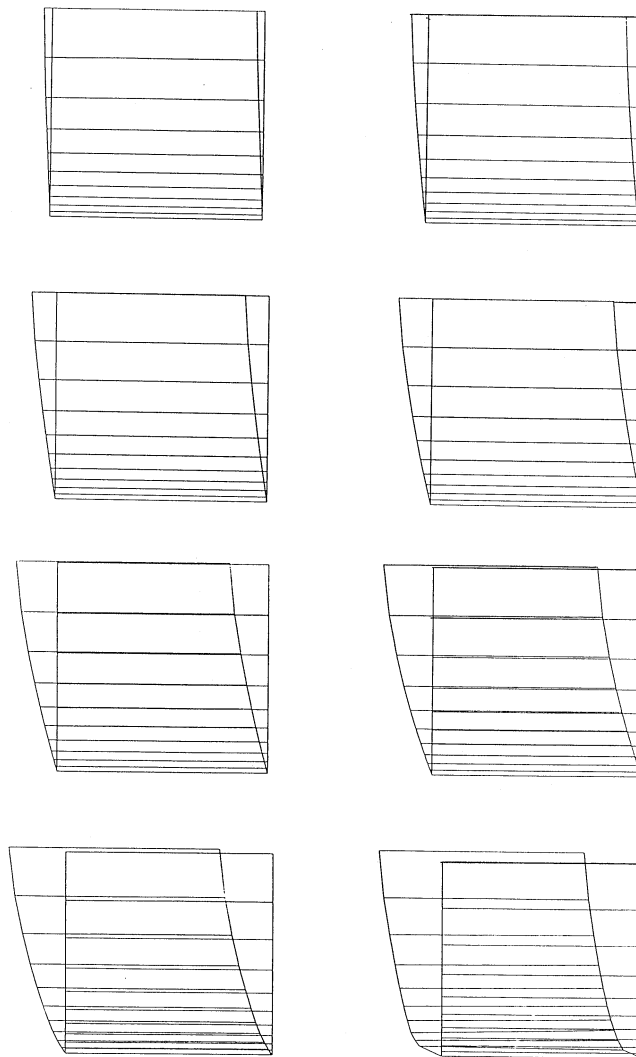


Figure 3. Evolution of the deformation of the mesh for the segment

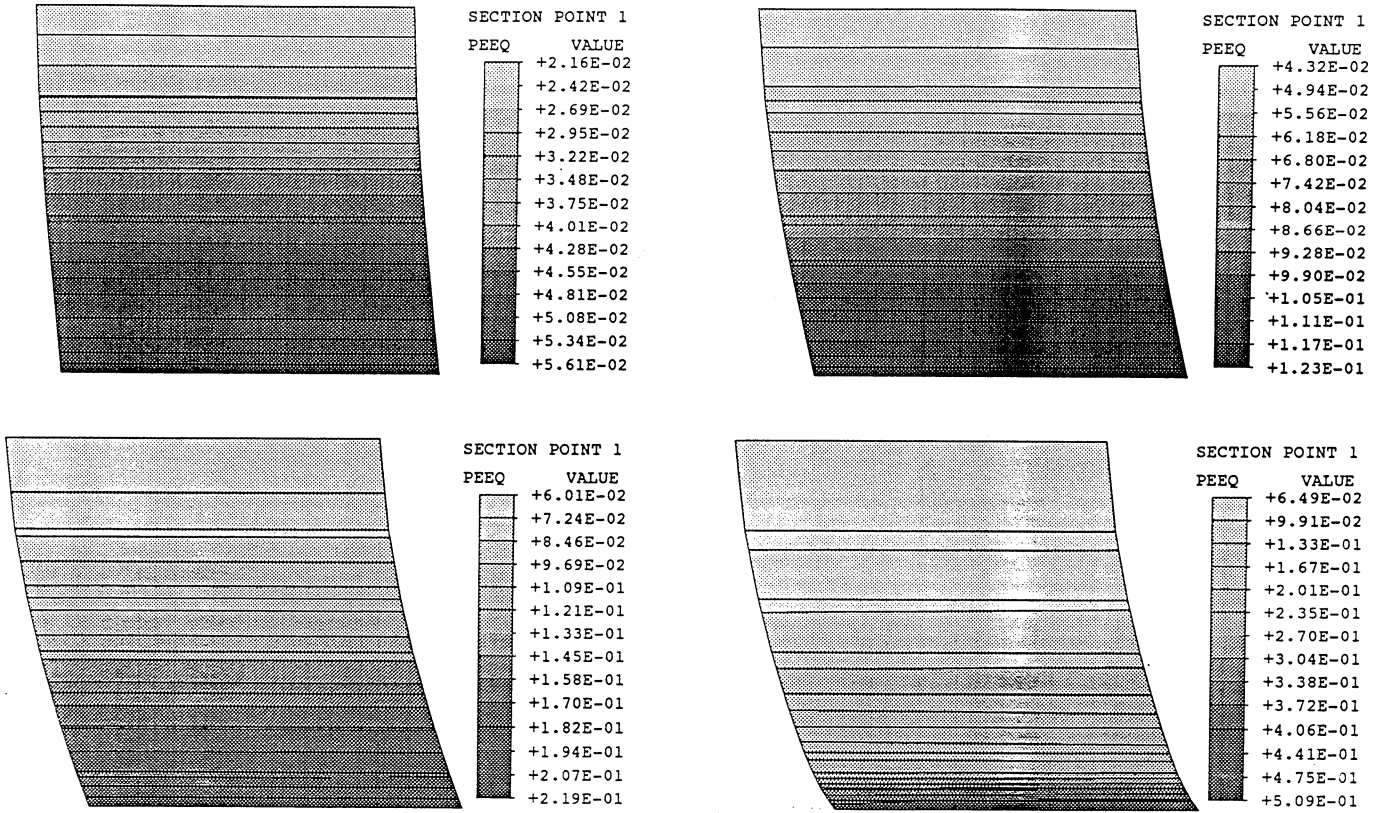


Figure 4. Evolution of the plastic equivalent strain in different laminates



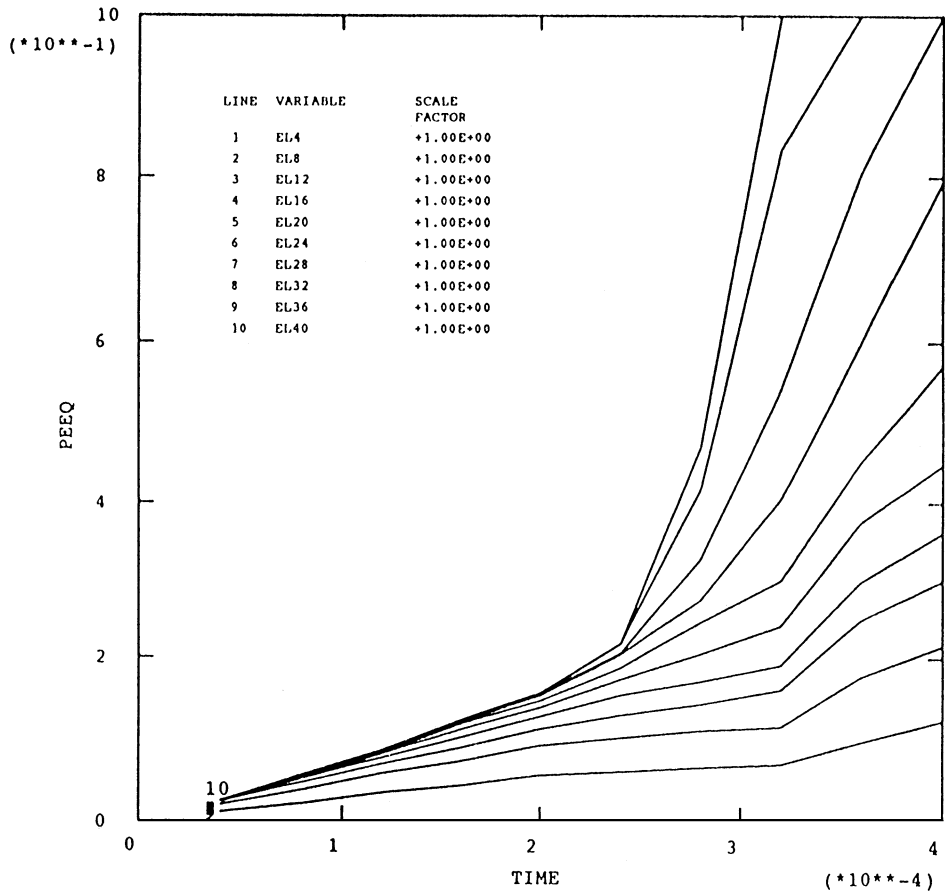


Figure 4. (Continued)

The following values for various material parameters are assumed (AISI 1018 cold roled steel)

$$\begin{aligned}
 \rho_M &= 7860 \text{ kg/m}^3 & c_p &= 460 \text{ J/(kg } ^\circ\text{C)}, & G &= 80 \text{ GPa}, \\
 K &= 210 \text{ GPa}, & \kappa_0 &= 237 \text{ MPa} & \kappa_1 &= 1.2 \kappa_0, \\
 \vartheta_0 &= 20^\circ\text{C}, & \xi_0 &= 0.001, & \xi^F &= 0.25, \\
 h &= \text{const} = 5.15, & n &= \text{const} = 1.25, & \chi^* &= 0.90, \\
 m &= 5 \text{ (for } \vartheta = 0), & T_m &= 2.5 \cdot 10^{-2} \text{ s (for } \vartheta = 0), \\
 m &= 4.7 \text{ (for } \vartheta = 80^\circ\text{C)}, & T_m &= 1.0 \cdot 10^{-2} \text{ s (for } \vartheta = 80^\circ\text{C)}.
 \end{aligned}$$

The tube has been twisted at nominal shear strain rate ranging  $10^3$ – $10^4 \text{ s}^{-1}$ .

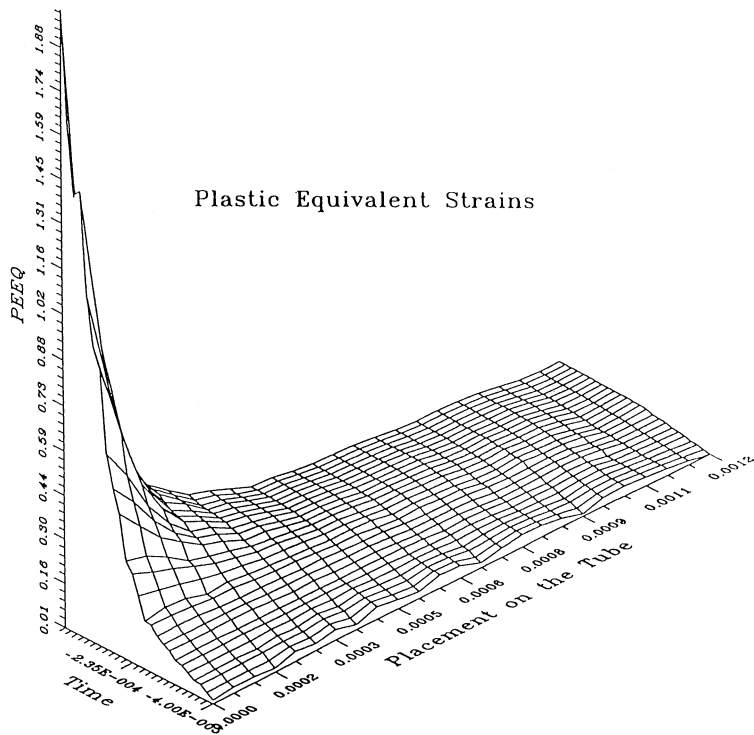


Figure 5. Plastic equivalent strain as a function of time and placement on the tube

For the particular example considered it has been assumed  $\dot{\xi} = 0$  (no influence of the micro-damage mechanism) and  $\omega_0^* = 253 \text{ s}^{-1}$ . The evolution of the deformation of the mesh for the segment is shown in Figure 3. In Figure 4 one can observe the evolution of the equivalent plastic deformation in different laminates and clear plastic strain localization effect around the mid cross section. The predicted width of this localized region is 0.2–0.3 mm, cf. Figure 5. The evolution of temperature in different laminates is presented in Figure 6 and for the segment in Figure 7. The maximum strain is of the order of 200 per cent and the temperature rise is of the order of  $150^\circ\text{C}$ .

The main result of this numerical simulation is the determination of a thin shear band region of finite width along the circumference of the tube which undergoes significant deformations and temperature rise. The predicted width of the determined shear band, the changes of temperature and deformation are in sufficiently good agreement with the experimental observations.<sup>1–4</sup>

It has been also found that the width of the shear band region and the temperature rise vary with the nominal strain rate as well as with the relaxation time assumed.

The evolution of the localized shear band region until occurrence of fracture has been simulated by Lodygowski and Perzyna.<sup>33</sup> In their study the influence of the micro-damage

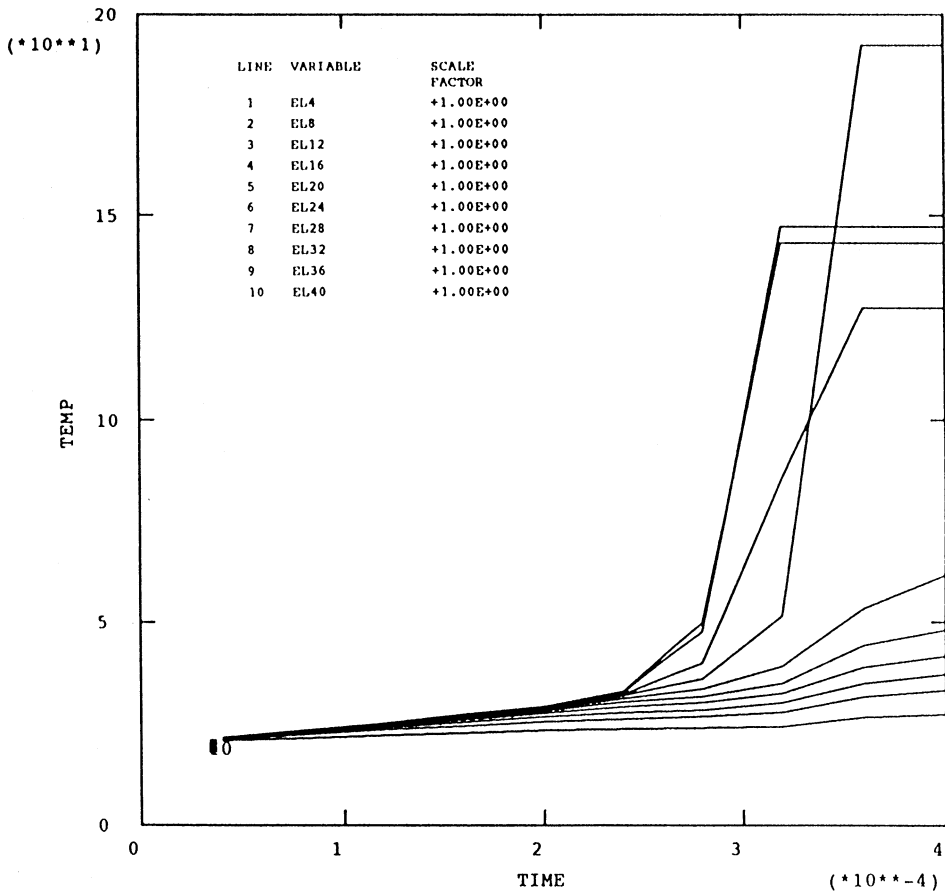


Figure 6. Evolution of the temperature rise in different laminates

mechanism has been taken into consideration. Particular forms of the material functions  $h^*$ ,  $g^*$ ,  $m^*$ ,  $\sigma_N$  and  $\sigma_{eq}$  which affect the micro-damage mechanism and have the influence on the final fracture of the tube have been postulated and discussed during the computation process. An exhaustive discussion of the results obtained and the comparison with the experimental observation data are also presented.

### 6. CONCLUSIONS

In the paper the problem of theoretical description and numerical simulation of the appearing and the development of plastic strain localization is discussed. The theory of thermo-viscoplasticity is used for the mathematical modelling and rate-dependent overstress viscoplasticity serves also as a mathematical method of regularization. The relaxation time of mechanical perturbations plays the role of regularization parameter which is important when dealing with materials exhibiting thermal softening. The viscosity allows the spatial differential operator in the governing equations to retain its ellipticity.

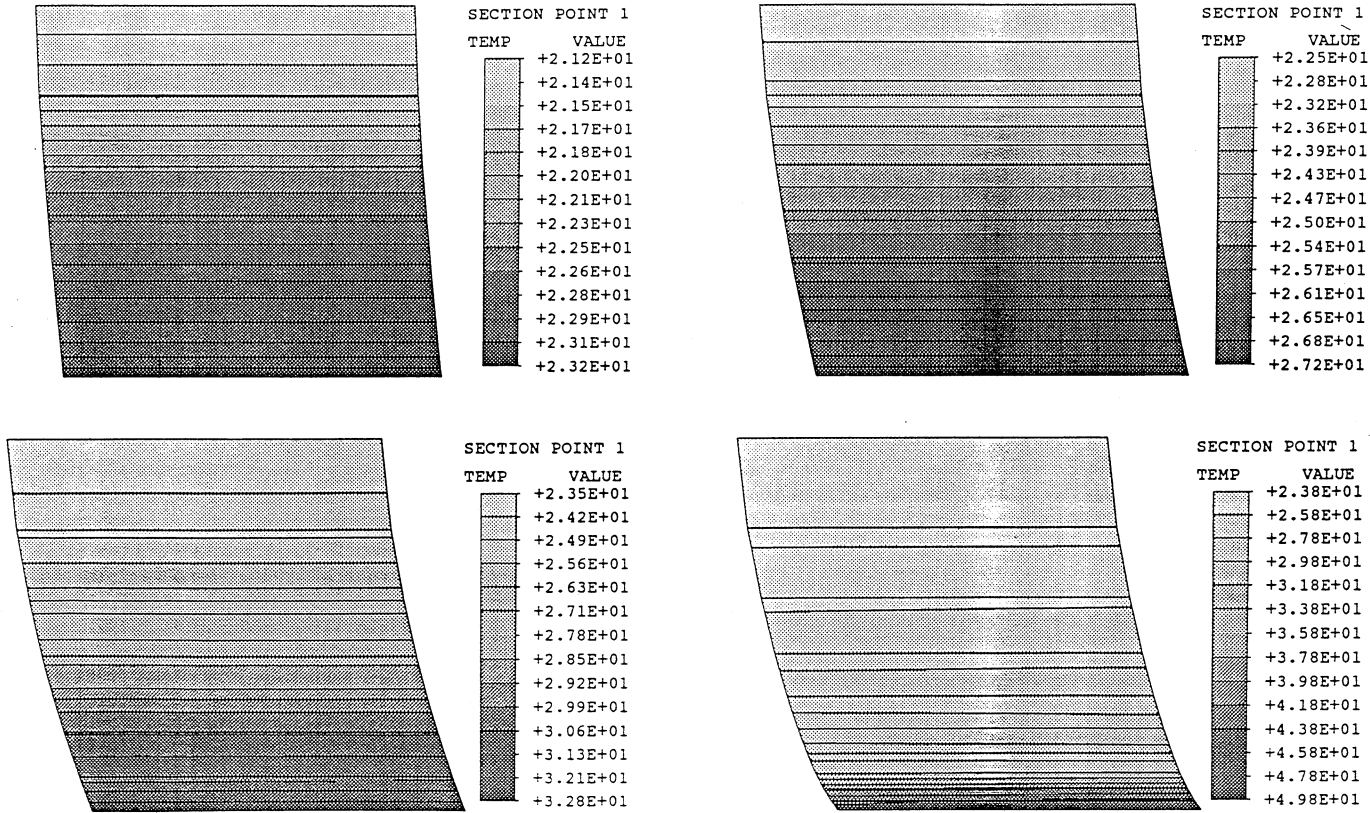


Figure 7. Evolution of temperature for the segment

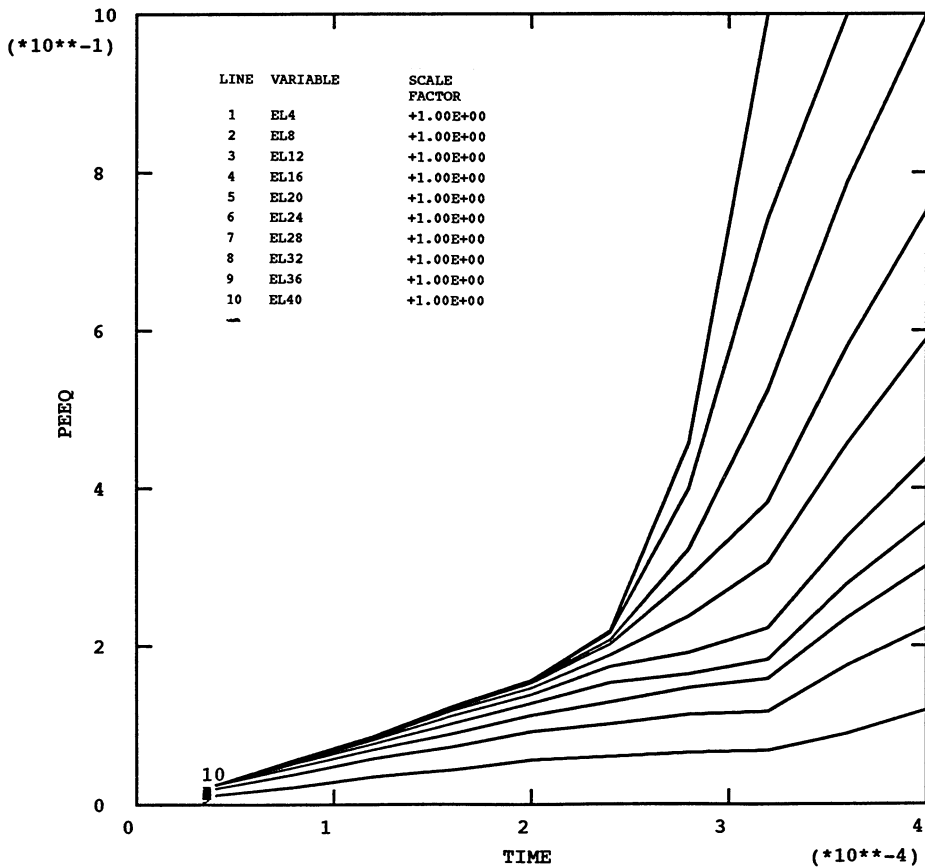


Figure 7. (Continued)

The attention was focussed on the well-posedness of the evolution problem and also on the convergence, consistency and stability of the discretized incremental problem.

The numerical examples are restricted to the numerical simulation of the twisting of a thin-walled tube in a split Hopkinson bar. The results of this adiabatic process were compared with the experiments of Duffy *et al.*<sup>1-4</sup> and showed a good qualitative and quantitative agreement.

ACKNOWLEDGEMENT

The paper has been prepared within the research programme sponsored by the Committee of Scientific Research under Grant 3 P 404 031 07.

REFERENCES

1. K. A. Hartley, J. Duffy and R. H. Hawley, 'Measurement of the temperature profile during shear band formulation in steels deforming at high strain rates', *J. Mech. Phys. Solids*, **35**, 283-301 (1987).

2. A. Marchand and J. Duffy, 'An experimental study of the formation process of adiabatic shear bands in a structural steel', *J. Mech. Phys. Solids*, **36**, 251–283 (1988).
3. A. Marchand, K. Cho and J. Duffy, 'The formation of adiabatic shear bands in an AISI 1018 cold-rolled steel', *Brown University Report*, 1988.
4. K. Cho, Y. C. Chi and J. Duffy, 'Microscopic observations of adiabatic shear bands in three different steels', *Brown University Report* (1989).
5. H. M. Zbib and J. S. Jurban, 'Dynamic shear banding: a three-dimensional analysis', *Int. J. Plasticity*, **8**, 619–641 (1992).
6. R. C. Batra and X. Zhang, 'On the propagation of a shear band in a steel tube', *J. Engng. Materials and Technology*, **116**, 155–161 (1994).
7. P. Perzyna, 'Instability phenomena and adiabatic shear band localization in thermoplastic flow processes', *Acta Mechanica*, **106**, 173–205 (1994).
8. P. Perzyna and M. K. Duszek-Perzyna, 'Phenomenological modelling of adiabatic shear band localization fracture of solids in dynamic loading processes', in M. H. Aliabadi, A. Carpinteri, S. Kalisky and D. J. Cartwright (eds.), *Localized Damage III: Computer-Aided Assessment and Control*, Computational Mechanics Publications, Southampton, 1994, pp. 579–588.
9. P. Perzyna, 'Interactions of elastic-viscoplastic waves and localization phenomena in solids', in J. L. Wegner and F. R. Norwood, (eds.), *IUTAM Symp. on Nonlinear Waves in Solids*, 1993, Victoria, Canada; ASME, New York, 1995, pp. 114–121.
10. J. A. Nemes and J. Eftis, 'Constitutive modelling on the dynamic fracture of smooth tensile bars', *Int. J. Plasticity*, **9**, 243–270 (1993).
11. L. J. Sluys, J. Block and R. de Borst, 'Wave propagation and localization in viscoplastic media', in D. R. J. Owen, E. Onate and E. Hinton (eds.), *Proc. 3rd Int. Conf. on Computational Plasticity, Fundamentals and Applications*, Barcelona, Pineridge Press, Swansea, 1992, pp. 539–550.
12. J. E. Marsden and T. J. R. Hughes, *Mathematical Foundations of Elasticity*, Prentice-Hall, Englewood Cliffs, N.J., 1983.
13. P. Perzyna, 'The constitutive equations for rate sensitive plastic materials', *Quart. Appl. Math.*, **20**, 321–332 (1963).
14. P. Perzyna, 'Thermodynamic theory of viscoplasticity', *Adv. Appl. Mech.*, **11**, 313–354 (1971).
15. P. Perzyna, 'Internal state variable description of dynamic fracture of ductile solids', *Int. J. Solids Struct.*, **22**, 797–818 (1986).
16. J. H. Mac Kenzie, 'The elastic constants of a solid containing spherical holes', *Proc. Phys. Soc.*, **63B**, 2–11 (1950).
17. D. A. Shockey, L. Seaman and D. R. Curran, 'The microstatistical fracture mechanics approach to dynamic fracture problem', *Int. J. Fracture*, **27**, 145–157 (1985).
18. D. R. Curran, L. Seaman and D. A. Shockey, 'Dynamic failure of solids', *Phys. Rep.*, **147**, 253–388 (1987).
19. J. N. Johnson, 'Dynamic fracture and spallation in ductile solids', *J. Appl. Phys.*, **52**, 2812–2825 (1981).
20. J. A. Nemes, J. Eftis and P. W. Randles, 'Viscoplastic constitutive modelling of high strain-rate deformation, material damage and spall fracture', *J. Appl. Mech.*, **57**, 282–291 (1990).
21. P. Perzyna and A. Drabik, 'Description of micro-damage process by porosity parameter for nonlinear viscoplasticity', *Arch. Mech.*, **41**, 895–908 (1989).
22. P. Perzyna and A. Drabik, 'Micro-damage mechanism in adiabatic processes', *Int. J. Plasticity* (1997) submitted for publication.
23. P. Perzyna, 'Constitutive modelling of dissipative solids for postcritical behaviour and fracture', *ASME, J. Eng. Mater. Technol.*, **106**, 410–419 (1984).
24. T. Lodygowski, 'On avoiding of spurious mesh sensitivity in numerical analysis of plastic strain localization', *CAMES*, **2**, 231–248 (1995).
25. P. Perzyna, 'Adiabatic shear band localization fracture of solids in dynamic loading processes', in J. Harding (eds.), *Proc. Int. Conf. on Mechanical and Physical Behaviour of Materials under Dynamic Loading*, Oxford, 1994, Les Editions de Physique Le Ulis, 1994, pp. 441–446.
26. T. R. J. Hughes, T. Kato and J. E. Marsden, 'Well-posed quasilinear second-order hyperbolic systems with applications to nonlinear elastodynamics and general relativity', *Arch. Rat. Mech. Anal.*, **63**, 273–294 (1977).
27. R. D. Richtmyer, *Principles of Advance Mathematical Physics*, Vol. I, Springer, New York, 1978.
28. R. Dautray and J.-L. Lions, *Mathematical Analysis and Numerical Methods for Science and Technology*, Vol. 6. *Evolution Problems II*. Springer, Berlin, 1993.
29. I. R. Ionescu and M. Sofonea, *Functional and Numerical Methods in Viscoplasticity*, Oxford University Press, Oxford, 1993.
30. R. D. Richtmyer and K. W. Morton, *Difference Methods for Initial-Value Problems*, Wiley, New York, 1967.
31. G. Strang and G. J. Fix, *An Analysis of the Finite Element Method*, Prentice-Hall, Englewood Cliffs, N.J., 1973.
32. A. Glema, W. Kakol and T. Lodygowski, 'A numerical modelling of adiabatic shear band formulation in a twisting test', *CAM&ES* (1997) submitted for publication.
33. T. Lodygowski and P. Perzyna, 'Localized fracture of inelastic polycrystalline solids under dynamic loading processes', *Int. J. Damage Mech.*, (1997), in print.
34. T. Lodygowski, M. Lengnick, P. Perzyna and E. Stein, 'Viscoplastic numerical analysis of dynamic plastic strain localization for a ductile material', *Archives Mech.*, **46**, 1–25 (1994).